University of Baghdad
College of Engineering
JOURNAL OF ENGINEERING

Journal of Engineering
journal homepage: www.jcoeng.edu.iq
Volume 31 Number 2 February 2025

Computerized Generation of Nonstandard and Asymmetric Involute Spur Gears Based on Rack Cutter Parametric Tracing

Ahmed A. Toman [1, 2, *], **Mohammad Q. Abdullah** [1]

[1]Department of Mechanical Engineering, College of Engineering, University of Baghdad, Baghdad, Iraq
[2]Department of Automobile Engineering, College of Engineering Al-Musayab, University of Babylon, Babylon, Iraq

ABSTRACT

In the field of gear design, to apply any form of analysis (such as FEA, dynamic, and stress analyses), a delicate and accurate representation of the gear geometry is essential. It is the foundation for any design modification attempts, and any approximation of the tooth profile must be avoided. In the literature, many approximations were held to the involute tooth geometry, particularly in the filet region, where it was simply represented by a straight line or circular arc instead of a true trochoidal arc from a generation process. This approach might lead to inaccurate bending stress results, as it fails to detect the impact of the undercut or the profile correction process. Other common approximations have been widely observed in the literature, such as utilizing an asymmetric cutter to simultaneously generate the two sides of the asymmetric gear. Moreover, the graphical rack-cutter generation technique was widely used to generate involute gears. This technique, although shown to be accurate in generating a 2D standard tooth, is time-consuming as it necessitates the use of source code, a programming language, a graphic processor for displaying computer graphs, a post-graphic processor for eliminating unrelated lines, and a post-process for exporting the tooth geometry to CAD software. This research presents an alternative direct computerized generation method that is shown to be accurate, generate both 2D and 3D gears, and be significantly more time-efficient. Moreover, a novel technique to generate a fully asymmetric nonstandard tooth (pressure angle, trochoidal fillet, and shifting factor) is proposed using two half-cutters.

Keywords: Generation, Involute spur gears, Nonstandard, Asymmetric, Rack-cutter

1. INTRODUCTION

Spur gears are commonly used in various mechanical systems for their efficient transmission of rotational motion and power **(Zhang and Mi, 2018)**. Even though early forms of gears

*Corresponding author
Peer review under the responsibility of University of Baghdad.
https://doi.org/10.31026/j.eng.2025.02.05

Article received: 20/06/2024
Article revised: 02/11/2024
Article accepted: 20/11/2024
Article published: 01/02/2025

were invented around the 18th century, the amount of attention and research dedicated to them has been continuously increasing due to the growing demand for improved performance and design refinements **(Barmina and Trubachev, 2021)**. Significant advancements in gear materials, surface finishes, and manufacturing quality have elevated gear performance to an impressive level **(Abdullah and Badri, 2011)**. Nonetheless, enhancing gear performance during the gear tooth design stage remains a comprehensive and effective approach **(Abdullah et al., 2015; Ismail and Abdullah, 2019; Toman and Abdullah, 2020)**.

Generating in gear cutting refers to the process of creating an involute curve using straight cutting edges on the cutter **(Ciornei et al., 2022)**. This results in a series of facets on the blank, forming the desired involute profile. The cutter and blank function as mating gears in contact during the cutting process. To produce gear teeth, generating methods leverage specific relative motion between the work gear and the cutter. These methods ensure theoretically correct gear tooth profiles, irrespective of the desired number of teeth on the gear. With a given diametral pitch, a single cutter can be used to cut gears with varying tooth counts, all of which will have theoretically accurate profiles and mesh interchangeably. The most commonly employed generating processes for gear teeth include the gear shaper process, rack cutter process, and hobbing process **(Gupta et al., 2017)**.

Reviewing the related literature, the rack cutter generation technique, one of the involute gear teeth generation methods, has been widely used to generate involute gears with standard and modified gear teeth and to study and investigate the performance of spur gears with various design modifications. **(Kapelevich, 2000)** introduced a graphical-based method for generating a spur gear with an asymmetric tooth. According to his method, the asymmetric gear tooth had to be generated via the use of an asymmetric rack-cutter by a generation process. **(Litvin et al., 2000)** introduced a stress and noise reduction gear design that uses an asymmetric pressure angle gear tooth (35,20 degrees) on the active and coast side and compared it with a (25) degree pressure angle gear tooth. An asymmetric rack-cutter was used to generate this asymmetric gear tooth based on a rack-cutter generation method. **(Yang, 2004)** introduced a mathematical model for generating asymmetric pinion and gear by using an asymmetric involute rack-cutter. According to the results, this model is capable of generating asymmetric gears with undercutting. **(Chen and Tsay, 2005)** introduced a method for designing and manufacturing small teeth number standard gears by adopting a modified rack-cutter. **(Fetvaci and Imrak, 2008)** used an asymmetric tooth rack-cutter to graphically generation the 2D profile of the asymmetric spur gear by conventional generation simulation. (**Hassan, 2008**; **Hassan, 2018**) reformulated the parametric equations for the trochoid and involute profiles for symmetric spur gears with standard and nonstandard (profile-shifted) teeth. The author developed a computer program using a programming language to plot the gear tooth profile. **(Bhosale and Ahmednagar, 2011)** adopted the FEM and 3D photo elasticity to analyze standard helical gear bending strength and compare the results with the Lewis equation. For the FEM investigation, the 3D models were modeled using CAD software (CATIA). **(Abdullah, 2012; Abdullah and Jweeg, 2012)** presented a group of geometrical modifications on the gear tooth profiles, such as asymmetric profiles with optimal fillet for both sides and by using an addendum modification, an alternative design approach was adopted to satisfy the best gear drive performance. The standard spur gear 2D models were graphically generated using a symmetric involute rack-cutter. On the other hand, half rack cutters were used to graphically generate each tooth side of the 2D gear models of non-standard spur gears. Fifteen points

were used to define the outer shape of the rack cutter. Then, the Cartesian coordinates of the geometrical points for the rack cutter were found. A mathematical simulation based on the principle of the gear shaping process with a rack-shaped cutter was adopted to generate the involute gear tooth profiles graphically and modified to consider tooth addendum modifications. **(Gupta et al., 2012)** studied the effect of the gear model on the maximum tooth contact stress for standard spur gears. The 3D gear models were generated using the (pro/Engineer) CAD software; then, these models were fed to a CAE software (ANSYS) for F.E. analysis. **(Masuyama et al., 2015; Masuyama and Miyazaki, 2016)** conducted 2D F.E. simulations to investigate the bending strength of spur gears with symmetric, asymmetric fillets and asymmetric pressure angle and fillet teeth. The 2D gear profiles and models were generated using symmetric and asymmetric rack-cutters utilizing the traditional rack-gear graphical rolling at the pitch circle. **(Rao and Vamsi, 2016)** studied the contact and shear stress of spur gears by FEM using CAE software (Ansys) and analytical investigation for different gear materials. The 3D models were formed by CAD software (Pro. E) then the geometry files were fed to FEM CAE software (Ansys). **(Hmoad, 2016; Hmoad and Abdullah, 2016)** conducted analytical, numerical (FEA), and photoelastic investigations to investigate the effect of using standard, asymmetric, and asymmetrically shifted symmetric pressure angle spur gear tooth profiles on sliding velocity behavior. The photoblastic gear models were fabricated utilizing CAM software. The geometry files required for the gear fabrication process and FEA were generated based on the rack-cutter generation method. The rack-cuter was divided into four parts (edges), and then the equations of each part were driven utilizing a coordinate transformation. The gear tooth 2D geometry was obtained by a simulation that involves utilizing shifting techniques to depict the relative motion between the cutter and the gear blank.

(Yılmaz et al., 2017) conducted a stress analysis on spur gears with a thin rim. The fillets of the investigated gear teeth were asymmetric of a trochoidal profile type. The gear 2D geometry was obtained utilizing an asymmetric rack-cutter. To generate this asymmetric gear tooth, the rack cutter was divided into six regions, and then a rack-cutter generation method was conducted based on Litvin's approach. In another work, **(Yılmaz et al., 2018)** conducted a stress analysis on spur gears with a thin rim. The pressure angles of the investigated gear teeth were asymmetric. The gear 2D geometry was obtained utilizing an asymmetric pressure angle rack-cutter employing the same rack-cutter generation method. **(Zhai et al., 2020)** presented a paramedic model for spur gears and an optimization method for the non-involute part of the tooth. (**Mo et al., 2024)** introduced a novel approach to designing cylindrical spur gears. By leveraging the unique properties of logarithmic spirals, the equation governing gear meshing was derived, enabling the determination of the conjugate tooth profile and the contact path for the gear pairs.

Ensuring precision in depicting the gear's geometry is crucial as it forms the fundamental basis for any attempts at making design modifications. Previous studies have widely employed the rack-cuter graphical generation method. However, the graphical rack-cutter generation method, although shown to be accurate in generating a standard tooth profile, is time-consuming. The output geometry files from this method, shown in **Fig. 1**, would require further processing by eliminating all the unnecessary lines produced from the reciprocal graphical motion between the cutter and the gear blank to obtain a clean 2D tooth geometry that might result in some profile errors. Furthermore, it will be complicated and time-consuming to process this geometry in CAD or CAE software to generate a 3D gear model.

Therefore, the main objectives of this research are:
1- Propose a computerized rack-cutter generation method as an alternative to the traditional graphical rack-cutter generation method. The proposed method is direct and efficient in terms of time, as it does not necessitate the use of a source code, a programming language, a graphic processor for displaying computer graphs, a post-graphic processor for eliminating unrelated lines and curves, or a post-process for exporting the tooth geometry to CAD software. Instead, it generates 2D and 3D gear geometries directly in the CAD software, utilizing a variety of modern CAD software capabilities. Thereby, this method facilitates the process of obtaining 3D spur gear models directly in the utilized CAD software, which is not directly feasible in the traditional graphical rack-cutter generation method.
2- Proposes novel techniques to generate asymmetric spur gears and fully asymmetric nonstandard spur gears.
3- Derive and reformulate the parametric equations for the tooth fillets and tooth involute profiles obtained from the parametric tracing of the reciprocal motion between the rack cutter and the gear blank to take into account the nonstandard gear tooth modifications, namely asymmetric fillets radii, asymmetric pressure angle, asymmetric profile shifting, and other combination of these nonstandard modifications.

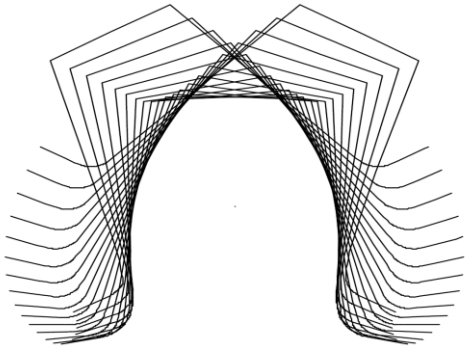

Figure 1. The output geometry of a spur gear is generated by a graphical rack-cutter generation method.

2. THE TRADITIONAL GRAPHICAL RACK-CUTTER GENERATION METHOD

The rack-cutter generation technique, one of the involute gear teeth generation methods, has been widely used to generate involute gears with standard and modified gear teeth**.** The rack-cutter generation technique is particularly important for creating 2D geometry profiles of spur gears. A rack can be defined as a particular type of gear with an infinitely large diameter. The curved sides of the gear gradually transition into straight sides. These sides are inclined at an angle equal to the standard pressure angle. In the traditional rack-cutter generation method, the rack-shaped cutting tool is usually geometrically represented by dividing it into several points or into regions (edge parts). The generation process is then carried out by rolling the whole rack cutter to the right and left directions from the initial position without slipping by incremental angles until a whole tooth shape is generated **(Davis, 2005)**, as illustrated in **Fig. 2**. In this process, the cutting tool (rack cutter) is given a shape conjugate with the form of the tooth to be cut and any geometrical modifications that are required on the gear tooth profiles must be done firstly on this rack cutter **(Hmoad, 2016)**.

This method, although shown to be accurate in generating a standard tooth profile, is time-consuming. The output geometry files from this method, shown in **Fig. 1**, would require further processing by eliminating all the unnecessary lines produced from the reciprocal graphical motion between the cutter and the gear blank to obtain a clean 2D tooth geometry that might result in some profile errors. Furthermore, it will be complicated and time-consuming to process this geometry in CAD or CAE software to generate a 3D gear model.

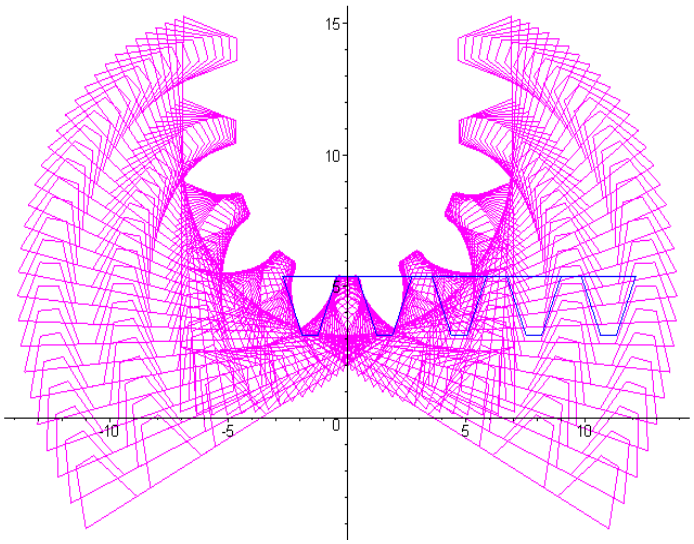

Figure 2. The generation process of a spur gear 2D geometry by the graphical rack-cutter generation method.

3. A COMPUTERIZED RACK CUTTER PARAMETRIC TRACING GENERATION METHOD

In this research, a computerized rack-cutter generation method is presented for the fast generation of standard and nonstandard 2D spur gear geometry with trochoidal arc fillets and involute profiles. A standardized hob or rack cutter is usually used to cut generated involute gears. Although the cutter's sharp tip corners will generate a trochoidal arc on the generated gear teeth in the fillet region, in practical application, the hob or rack cutter will have a rounded tip corner by an amount of r_f , instead of sharp corners **(Lynwander, 1983)**, as shown in **Fig. 3**. The generation process of a standard spur gear by a straight-sided cutting tool (hob or basic rack) is shown in **Fig. 4**. When the tool, shown in **Fig. 3**, move a transverse distance by amount of $(c + p)$, the gear blank rotate by an amount of $(\frac{(c+p)}{R_p})$ **(Lynwander, 1983)**. In the traditional graphical generation method, depicted in **Fig. 5**, numerous lines are produced due to the interaction between the cutter and the workpiece during the simulation of the cutting process's kinematics. These lines represent the outer boundary of the cutter at each relative motion interval. However, the crucial points are the intersections of the cutter's outer boundary lines, which represent the involutes and trochoidal profiles that create the tooth profile **(Fetvaci, 2012)**. By tracing the motion of the straight-sided cutter with its rounded corners tip, we can drive the parametric equations that represent the involutes and trochoidal profiles, which highly facilitate the generation process of the gear tooth profile **(Lynwander, 1983)**. These parametric equations can then be easily programmed in modern CAD software to generate a precise 3D gear model by feeding them with the required design specifications of any desired gear.

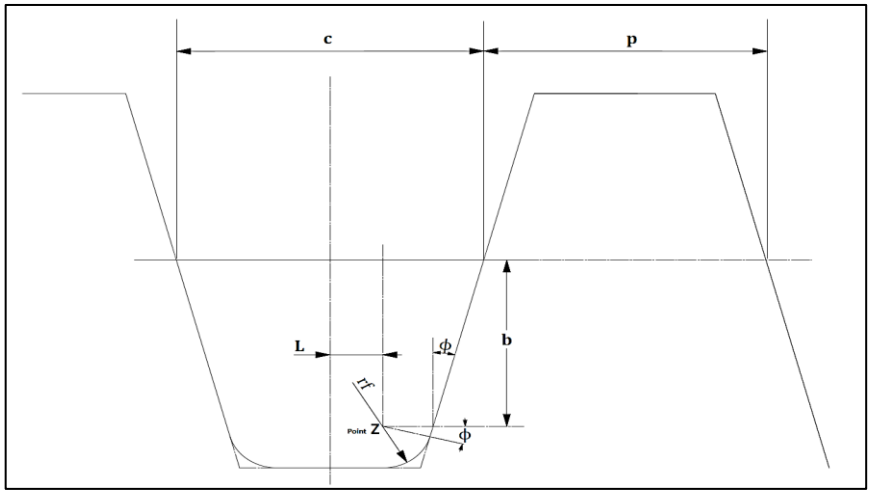

Figure 3. The basic rack-cutter geometry with round tip corners **(Lynwander, 1983).**

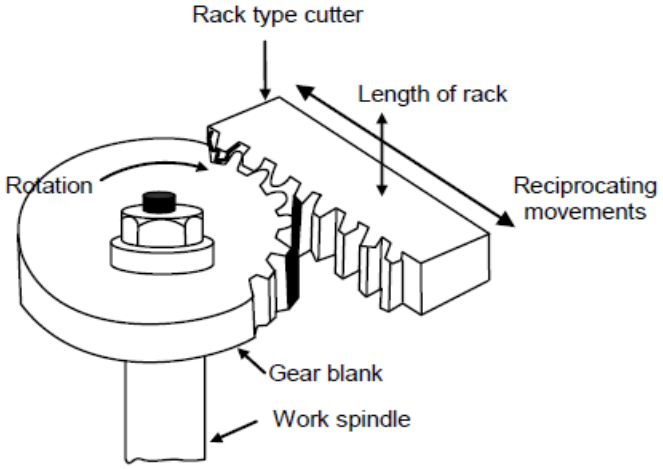

Figure 4. The generation process of a spur gear tooth by a rack-cutter **(Shaoyan and Yufu, 2022).**

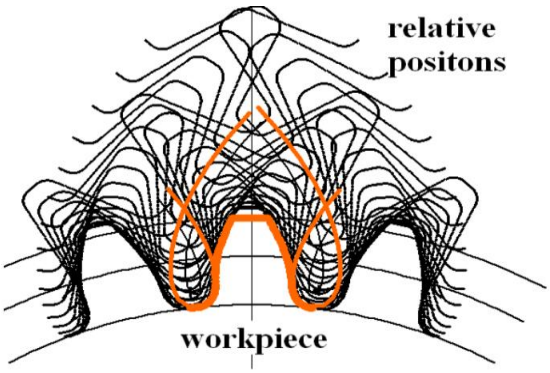

Figure 5. The involute and trochoidal profiles are generated by the graphical rack-cutter generation method **(Fetvaci 2012)**.

3.1 The Parametric Equations for the Involute Portion of the Gear Flank

When the desired gear pressure angle is identified, the involute function (Θ) and the base circle radius (R_b) can be easily then calculated. The x and y coordinate at any radius R can be found if the thickness of the gear tooth at that radius R is determined. The coordinates of the involute curve when the y-axis at the tooth center can be found as follows:
From **Fig. 6**, if the radius R_s Is equal to the pitch radius **(Ugural, 2022)**:

$$R_s = R_p = R_G = \frac{mz}{2} \quad (1)$$
$$\phi_s = \phi \quad (2)$$
$$inv\ \phi_s = (\tan\phi_s - \phi_s) = (tan\ \phi - \phi) \quad (3)$$
$$R_b = R_p * cos\ (\phi) \quad (4)$$

The gear tooth thickness (t) is equal to the cutter space thickness (p), and for a standard tooth, the tooth thickness(t) and space thickness(s) are equal, at R_p It is given by **(Colbourne, 1987)**,

$$t_s = p = s_s = c = \frac{\pi m}{2} \quad (5)$$

Referring to **Fig. 6,** the angle (γ) is equal to:

$$\gamma = inv\ \phi_s + \frac{t_s}{2R_p} \quad (6)$$

Since the tooth thickness at R_p can be directly evaluated, the thickness t_RAt any radius, R can be evaluated as follows **(Colbourne, 1987)**:
Referring to **Fig. 6**, we can see that:

$$inv\ \phi_R = (\tan\phi_R - \phi_R) \quad (7)$$
$$\phi_R = \cos^{-1}(\frac{R_b}{R}) \quad \text{i.e.} \quad R = \frac{R_b}{\cos\phi_R} \quad (8)$$

$$t_R = R\left[\left(\frac{t_s}{R_p}\right) + 2inv\ \phi_s - 2inv\ \phi_R\right] \quad (9)$$

$$\theta_R = \gamma - inv\ \phi_R = \left[inv\ \phi_s + \frac{t_s}{2R_p} - inv\ \phi_R\right] \quad (10)$$

The x and y coordinates of the involute profile are **(Buckingham, 2011)**:

$$x = R\sin(\theta_R) \quad (11)$$
$$y = R\cos(\theta_R) \quad (12)$$

For a standard gear tooth:
The angle θ_R Can be evaluated by substituting Eqs. (1), (3), (5), and (7) in Eq. (10):

$$\theta_R = \left[(tan\ \phi - \phi) + \frac{\pi}{2z} - \tan\phi_R + \phi_R\right] \quad (13)$$

As a result, the parametric equations for the standard tooth's left and right sides are as follows:

$$x_{l,r} = \frac{mz\cos\phi}{2\cos\lambda}\sin\left(\pm(\tan\phi - \phi) \pm \frac{\pi}{2z} \mp (\tan\lambda - \lambda)\right) \quad (14)$$
$$y_{l,r} = \frac{mz\cos\phi}{2\cos\lambda}\cos\left(\pm(tan\ \phi - \phi) \pm \frac{\pi}{2z} \mp (tan\ \lambda - \lambda)\right) \quad (15)$$

Where the symbol λ represents the angle of rotation, to generate an involute profile, its value ranges from zero to one radian, and it is equal to the angle. ϕ_R. In the above equations and what follows, the upper signs are for the left/loaded side, and the lower ones are for the right/unloaded side.

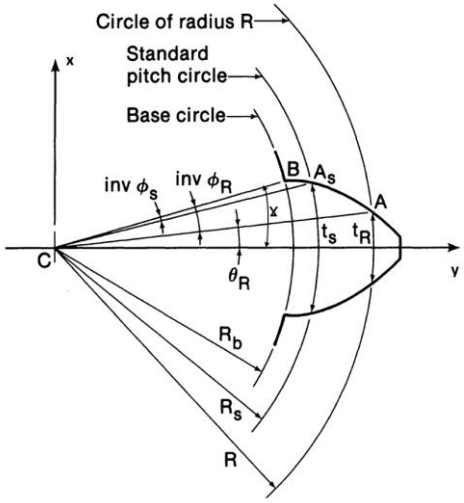

Figure 6. The determination of gear tooth thickness **(Colbourne, 1987).**

3.2 The Parametric Equations For the Trochoidal Arc Fillet Portion of the Gear Flank

As mentioned earlier in **Fig. 4**, when the cutter (**Fig. 3**) translates by a$(c + p)$, the gear blank rotates by a $\left(\frac{(c+p)}{R_p}\right)$ .This angle, as illustrated in **Fig. 7**, is equal to **(Mitchiner and Mabie, 1982; Lynwander, 1983)**:

$$\left(\frac{(c+p)}{R_p}\right) = 2(w + v) \quad (16)$$

Referring to **Fig. 3** and **Fig. 7**, we can find the angles (v and w) as follows:

$$v = L/R_p \quad (17)$$

$$w = \frac{\left[\frac{(c+p)}{2} - L\right]}{R_G} \quad (18)$$

Where for a standard gear tooth **(Mitchiner and Mabie, 1982; Lynwander, 1983)**:

$$L = \frac{c}{2} - b\tan\phi - \frac{r_f}{\cos\phi} \quad (19)$$

$$b = h_d - r_f \quad (20)$$

$$r_{f=}r_{f_f}.m \quad (21)$$

$$h_{d=}h_{d_f}.m \quad (22)$$

Fig. 8 shows A trochoidal profile generated by the center point of the rack-cutter rounded tip (Z), the gear blank rotates by an angle(E), due to the translation motion of the rack-cuter by an amount of ($R_G E$). Which can be represented by **(Lynwander, 1983)**:

$$X_Z = R_Z \sin(T - E) = R_Z(sinTcosE - cosTsinE) \quad (23)$$

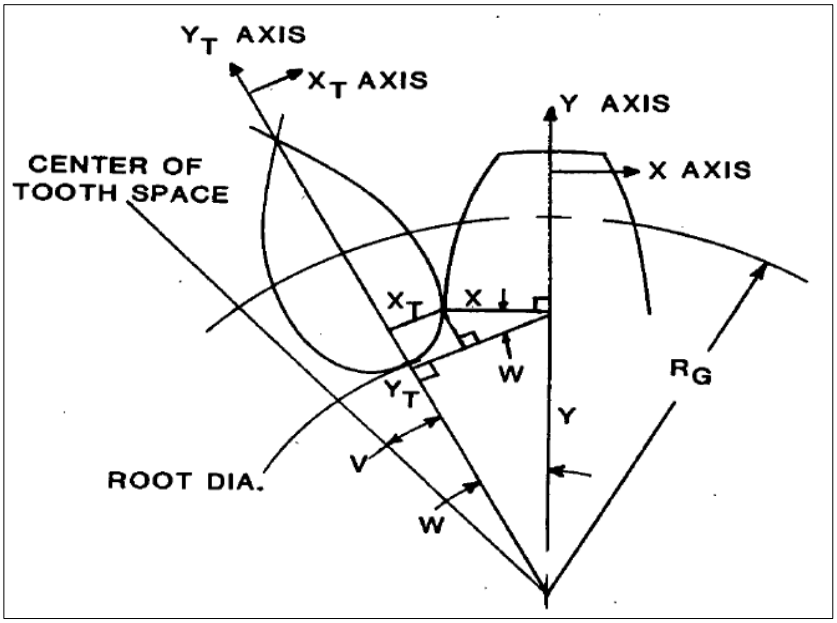

Figure 7. A spur gear tooth profile is generated by a rack-cutter **(Lynwander, 1983).**

$$Y_Z = R_Z \cos(T - E) = R_Z(cosTsinE - sinTcosE) \quad (24)$$

Since:

$$\cos(T) = (R_G - b)/R_Z \quad (25)$$

$$\sin(T) = (R_G\ b)/R_Z \quad (26)$$

By substituting Eqs. (25) and (26) into Eqs. (23) and (24), respectively, we get **(Lynwander, 1983)**:

$$X_Z = [(R_G E)\ cosE - (R_G - b)\ sinE] \quad (27)$$

$$Y_Z = [(R_G E)\ sinE + (R_G - b)\ cosE] \quad (28)$$

Now, to get the trochoidal arc generated by the rounded corners of the rack tip by a radius. r_f, by referring to **Fig. 9,** the true trochoidal arc coordinates about its local coordinate system are **(Lynwander, 1983)**:

$$X_T = X_Z + Rcos(\Lambda) \quad (29)$$

$$Y_T = Y_Z\ - Rsin(\Lambda) \quad (30)$$

where **Λ** equals:

$$\Lambda = dX_Z/dY_Z \quad (31)$$

By finding dX_Z/dE and dY_Z/dE angle **Λ** can be found, as follows **(Lynwander, 1983)**:

$$\frac{dX_Z}{dE} = [-(R_G E)\sin(E) + R_G\cos(E) - R_G cos(E) + b\cos(E)] \quad (32)$$

$$\frac{dY_Z}{dE} = [-R_G \sin(E) + b\sin(E) + [R_G E co\ s(E)] + R_G \sin(E)] \quad (33)$$

By applying a coordinate transformation to Eqs. (29) and (30), the Cartesian coordinates in the general global (X, Y) system can be found, as illustrated in **Fig. 7**, as follows **(Lynwander, 1983)**:

$$\sin(w) = [(X_T + X\cos(w))/Y] \quad (34)$$
$$\cos(w) = [(Y_T - X\sin(w))/Y] \quad (35)$$

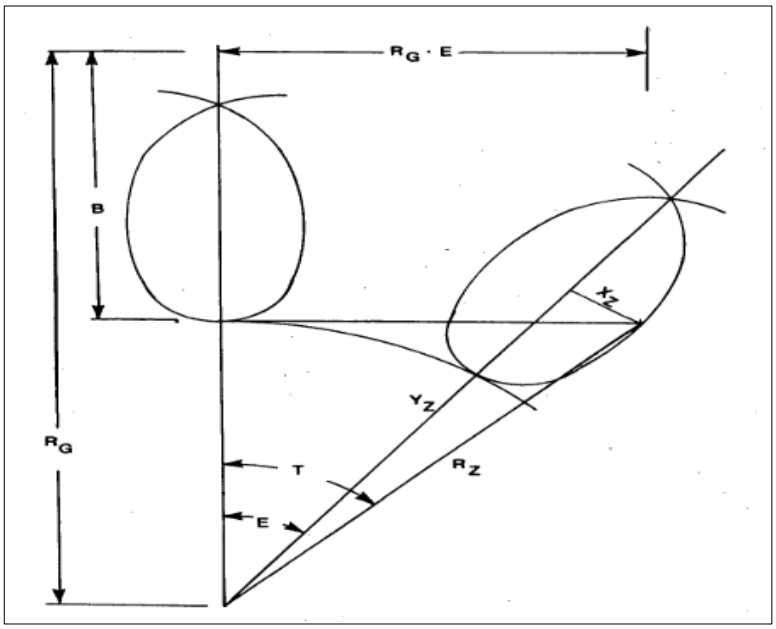

Figure 8. A trochoidal profile is generated by the center point of the rack-cutter rounded tip (Z) **(Lynwander, 1983).**

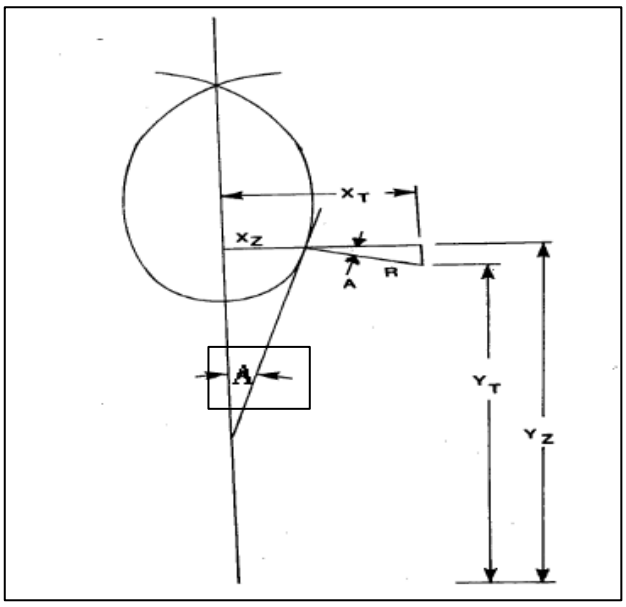

Figure 9. The trochoidal profile coordinates are generated by the rounded tip of the cutter in the global coordinate system **(Lynwander, 1983).**

From Eqs. (34) and (35), we get:

$$(X_T + X\,cos(w))/\,sin(w) = [(Y_T - X\sin(w))/\,cos(w)] \quad (36)$$

Hence:

$$X_T\,cos(w) + X\cos^2(w) = Y_T\,sin(w) - X\,sin^2(w) \quad (37)$$

Therefore:

$$X = Y_T\sin(w) - X_T\,cos(w) \quad (38)$$

$$Y = Y_T\,cos(w) + X_T\,sin(w) \quad (39)$$

$$\Lambda = \{\tan^{-1}(\frac{[-(R_G\,E)\sin(E)+b\cos(E)]}{[-R_G\,sin(E)+b\,sin(E)+[R_G E\cos(E)]+R_G\sin(E)]})\} \quad (40)$$

Finally, by substituting the equations from Eq. (17) to (40), we get the parametric equations for the left and right trochoidal arc fillet portions of the gear tooth:

$$x_{l,r} = \left[\frac{\text{mz}\,\psi\sin(\psi)}{2} + \left(\frac{m\left(z-2(h_{df}-r_{ff})\right)}{2}\right)\cos(\psi) - \left\{r_{ff}m\sin\left(\tan^{-1}\left(\frac{(h_{df}-r_{ff})\cos(\psi)-\frac{z\psi\,sin(\psi)}{2}}{(h_{df}-r_{ff})\sin(\psi)-\frac{z\psi\,cos(\psi)}{2}}\right)\right)\right\}\right]\sin\left(\pm 2\left(\frac{\frac{\pi}{4}+(h_{df}-r_{ff})\tan(\phi)+\frac{r_{ff}}{\cos(\phi)}}{z}\right)\right) \mp \left[\frac{\text{mz}\,\psi\cos(\psi)}{2} - \left(\frac{m\left(z-2(h_{df}-r_{ff})\right)}{2}\right)\sin(\psi) + r_{ff}m\cos\left\{\tan^{-1}\left(\frac{(h_{df}-r_{ff})\cos(\psi)-\frac{z\psi\,sin(\psi)}{2}}{(h_{df}-r_{ff})\sin(\psi)-\frac{z\psi\,cos(\psi)}{2}}\right)\right\}\right]\cos\left(\pm 2\left(\frac{\frac{\pi}{4}+(h_{df}-r_{ff})\tan(\phi)+\frac{r_{ff}}{\cos(\phi)}}{z}\right)\right) \quad (41)$$

$$y_{l,r} = \left[\frac{\text{mz}\,\psi\sin(\psi)}{2} + \left(\frac{m\left(z-2(h_{df}-r_{ff})\right)}{2}\right)\cos(\psi) - \left\{r_{ff}m\sin\left(\tan^{-1}\left(\frac{(h_{df}-r_{ff})\cos(\psi)-\frac{z\psi\,sin(\psi)}{2}}{(h_{df}-r_{ff})\sin(\psi)-\frac{z\psi\,cos(\psi)}{2}}\right)\right)\right\}\right]\cos\left(\pm 2\left(\frac{\frac{\pi}{4}+(h_{df}-r_{ff})\tan(\phi)+\frac{r_{ff}}{\cos(\phi)}}{z}\right)\right) \pm \left[\frac{\text{mz}\,\psi\cos(\psi)}{2} - \left(\frac{m\left(z-2(h_{df}-r_{ff})\right)}{2}\right)\sin(\psi) + r_{cf}m\cos\left\{\tan^{-1}\left(\frac{(h_{df}-r_{ff})\cos(\psi)-\frac{z\psi\,sin(\psi)}{2}}{(h_{df}-r_{ff})\sin(\psi)-\frac{z\psi\,cos(\psi)}{2}}\right)\right\}\right]\sin\left(\pm 2\left(\frac{\frac{\pi}{4}+(h_{df}-r_{ff})\tan(\phi)+\frac{r_{ff}}{\cos(\phi)}}{z}\right)\right) \quad (42)$$

Where the symbol ψ represents the generation angle, and its value can be taken from zero to one radian, and it is equal to the angle E. The important part of the trochoidal arc that we are interested in is the part that is tangent to the dedendum circle and tangent to the involute curve at the limit diameter **(Radzevich, 2017)**, which represents the generated gear filet.

3.3 Asymmetric Spur Gear Tooth Generation

Asymmetric gears have different pressure angles on the active and coast sides **(Kapelevich, 2018)**, and because of that, the rolling angle of the generation cutter will have different values for each side, which means that it should not be generated similarly to the symmetric standard gears case, i.e. not by just replacing the symmetric generation tool (hob or rack) with an asymmetric one **(Abdullah, 2012; Abdullah and Jweeg, 2012)**. Therefore, the technique to generate true asymmetric tooth profiles is by using two half-cutters, which have different pressure angle values (and can also have different fillet radii), so each half will be used to generate one half of the desired asymmetric tooth (either the active or coast side), as illustrated in **Fig. 10**.

The dimensions are the same as in the case of standard gear, except for the following dimensions, which have different values for each tooth side:

$$R_{bl,u} = R_p \cos(\phi_{l,u}) \tag{43}$$

$$r_{fl,u} = r_{ffl,u}\, m \tag{44}$$

$$b_{l,u} = hd - r_{fl,u} \tag{45}$$

$$L_{l,u} = \frac{c}{2} - b_{l,u} \tan(\phi_{l,u}) - \frac{r_{fl,u}}{\cos(\phi_{l,u})} \tag{46}$$

$$w_{l,u} = \frac{(c+p) - L_{l,u}}{2R_p} \tag{47}$$

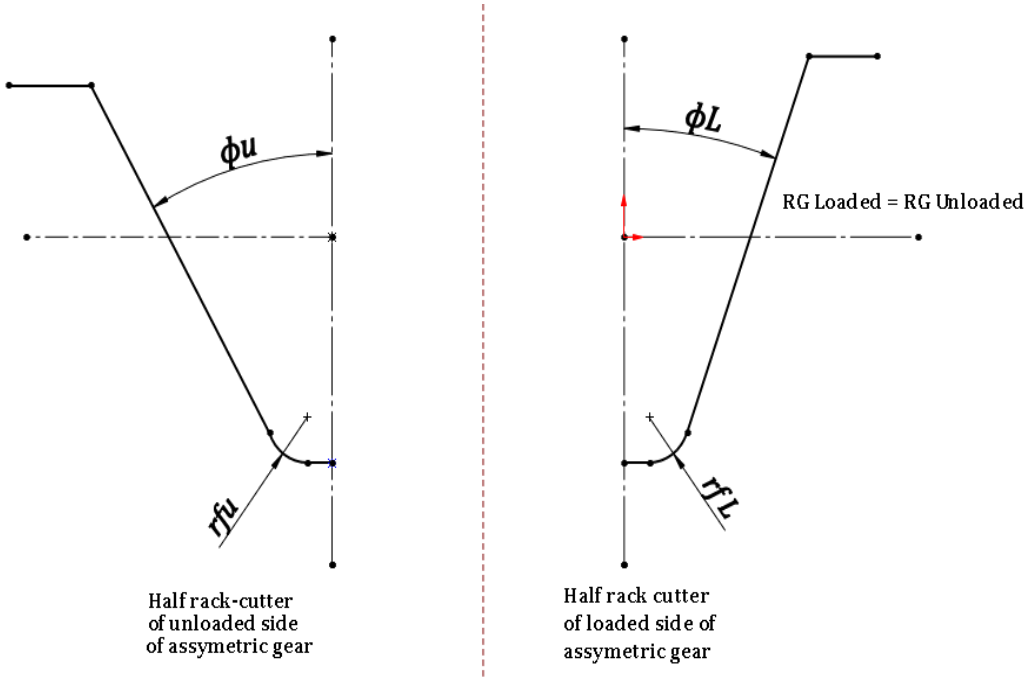

Figure 10. The loaded and unloaded half rack cutters for the generation technique of asymmetric gear tooth.

The generation parametric equations for the involutes and trochoidal fillet profiles then have the following form for each side of the tooth:

For the involute profiles:

$$x_{l,u} = \frac{mz \cos\phi_{l,u}}{2\cos\lambda} \sin\left(\pm[\tan\phi_{l,u} - \phi_{l,u}] \pm \frac{\pi}{2z} \mp [tan\,\lambda - \lambda]\right) \tag{48}$$

$$y_{l,u} = \frac{mz \cos\phi_{l,u}}{2\cos\lambda} \cos\left(\pm[\tan\phi_{l,u} - \phi_{l,u}] \pm \frac{\pi}{2z} \mp [tan\,\lambda - \lambda]\right) \tag{49}$$

For the trochoidal fillet profiles:

$$x_{l,u} = \left[\frac{\text{mz}\,\psi\sin(\psi)}{2} + \left(\frac{m\left(z-2\left(h_{df}-r_{ffl,u}\right)\right)}{2}\right)\cos(\psi) - \left\{r_{ffl,u}m\sin\left(\tan^{-1}\left(\frac{(h_{df}-r_{ffl,u})\cos(\psi)-\frac{z\psi\,\sin(\psi)}{2}}{(h_{df}-r_{ffl,u})\sin(\psi)-\frac{z\psi\,\cos(\psi)}{2}}\right)\right)\right\}\right]\sin\left(\pm 2\left(\frac{\frac{\pi}{4}+(h_{df}-r_{ffl,u})\tan(\phi_{l,u})+\frac{r_{ffl,u}}{\cos(\phi_{l,u})}}{z}\right)\right) \mp \left[\frac{\text{mz}\,\psi\cos(\psi)}{2} - \left(\frac{m\left(z-2\left(h_{df}-r_{ffl,u}\right)\right)}{2}\right)\sin(\psi) + r_{ffl,u}m\cos\left\{\tan^{-1}\left(\frac{(h_{df}-r_{ffl,u})\cos(\psi)-\frac{z\psi\,\sin(\psi)}{2}}{(h_{df}-r_{ffl,u})\sin(\psi)-\frac{z\psi\,\cos(\psi)}{2}}\right)\right\}\right]\cos\left(\pm 2\left(\frac{\frac{\pi}{4}+(h_{df}-r_{ffl,u})\tan(\phi_{l,u})+\frac{r_{ffl,u}}{\cos(\phi_{l,u})}}{z}\right)\right) \quad (50)$$

$$y_{l,u} = \left[\frac{\text{mz}\,\psi\sin(\psi)}{2} + \left(\frac{m\left(z-2\left(h_{df}-r_{ffl,u}\right)\right)}{2}\right)\cos(\psi) - \left\{r_{ffl,u}m\sin\left(\tan^{-1}\left(\frac{(h_{df}-r_{ffl,u})\cos(\psi)-\frac{z\psi\,\sin(\psi)}{2}}{(h_{df}-r_{ffl,u})\sin(\psi)-\frac{z\psi\,\cos(\psi)}{2}}\right)\right)\right\}\right]\cos\left(\pm 2\left(\frac{\frac{\pi}{4}+(h_{df}-r_{ffl,u})\tan(\phi_{l,u})+\frac{r_{ffl,u}}{\cos(\phi_{l,u})}}{z}\right)\right) \pm \left[\frac{\text{mz}\,\psi\cos(\psi)}{2} - \left(\frac{m\left(z-2\left(h_{df}-r_{ffl,u}\right)\right)}{2}\right)\sin(\psi) + r_{ffl,u}m\cos\left\{\tan^{-1}\left(\frac{(h_{df}-r_{ffl,u})\cos(\psi)-\frac{z\psi\,\sin(\psi)}{2}}{(h_{df}-r_{ffl,u})\sin(\psi)-\frac{z\psi\,\cos(\psi)}{2}}\right)\right\}\right]\sin\left(\pm 2\left(\frac{\frac{\pi}{4}+(h_{df}-r_{ffl,u})\tan(\phi_{l,u})+\frac{r_{ffl,u}}{\cos(\phi_{l,u})}}{z}\right)\right) \quad (51)$$

3.4 Corrected and Negative Profile Shifted Asymmetric Spur Gear Generation

To generate corrected (positive shifted) and negative profile shifted symmetric or asymmetric spur gears (nonstandard gears), the generation tool (hob or rack cutter reference line) should be shifted by a positive or negative amount (x) from the generation radius **(Hmoad, 2016)**. The resulting gears will be nonstandard and operate at a different center distance. In the case of profile shifted asymmetric gears generation, with symmetric or asymmetric shift factor(s), two half-rack cutters have been used to generate the tooth profile, so, as in the case of unshifted asymmetric gears generation technique, each half-cutter has been used to generate one half of the gear tooth. Nonstandard shifted gears have two distinct sets of dimensions: corrected (generation) dimensions, which remain constant despite the gear ratio, and operating dimensions, which vary with the gear ratio, as provided below corrected dimensions **(Ugural, 2022):**

$$R_G = R_p = \frac{mz}{2} \quad (52)$$
$$h_{ac} = (h_{af}\,m) + (x\,m) \quad (53)$$
$$h_{dc} = \left(h_{df}\,m\right) - (x\,m) \quad (54)$$
$$R_{ac} = R_{aw} = R_p + h_{ac} \quad (55)$$
$$R_{dc} = R_{dw} = R_p - h_{dc} \quad (56)$$
$$R_{bc} = R_{bw} = R_b = R_p\cos\phi \quad (57)$$
$$c_c = s_{sc} = \left(\frac{\pi m}{2}\right) - (2\,x.m.\tan\phi) \quad (58)$$
$$p_c = t_{sc} = \left(\frac{\pi m}{2}\right) + (2\,x\,.m.tan\,\phi) \quad (59)$$
$$b_c = h_{dc} - r_f \quad (60)$$

$$L_c = \frac{c_c}{2} - b_c \tan(\phi) - \frac{r_f}{\cos(\phi)} \quad (61)$$

$$w_c = \frac{\left(\left(\frac{c_c+p_c}{2}\right)-L_c\right)}{R_G} \quad (62)$$

Working (operating) dimensions **(Risitano, 2011):**

$$(\tan\phi_w - \phi_w) = \frac{2(x_{l1}+x_{l2})\tan\phi}{Z_1+Z_2} + (\tan\phi - \phi) \quad (63)$$

$$R_{pw} = R_p \frac{\cos\phi}{\cos\phi_w} \quad (64)$$

$$R_{bw} = R_{pw}\cos\phi_w = R_p\cos\phi = R_{bc} = R_b \quad (65)$$

$$h_{aw} = R_{aw} - R_{pw} \quad (66)$$

$$h_{dw} = R_{pw} - R_{dw} \quad (67)$$

The generation parametric equations for the involutes and trochoidal fillet profiles then have the following form for each side of a fully asymmetric tooth:

For the involute profiles:

$$x_{l,u} = \frac{mz\cos\phi_{l,u}}{2\cos\lambda}\sin\left(\pm[\tan\phi_{l,u} - \phi_{l,u}] \pm \frac{2x_{l,u}\tan\phi_{l,u}}{z} + \frac{\pi}{2z} \mp [tan\,\lambda - \lambda]\right) \quad (68)$$

$$y_{l,u} = \frac{mz\cos\phi_{l,u}}{2\cos\lambda}\cos\left(\pm[\tan\phi_{l,u} - \phi_{l,u}] \pm \frac{2x_{l,u}\tan\phi_{l,u}}{z} \pm \frac{\pi}{2z} \mp [tan\,\lambda - \lambda]\right) \quad (69)$$

For the trochoidal fillet profiles:

$$x_{l,u} = \left[\frac{\text{mz}\,\psi\sin(\psi)}{2} + \left(\frac{m\left(z-2\left(h_{df}-x_{l,u}-r_{ffl,u}\right)\right)}{2}\right)\cos(\psi) - \left\{r_{ffl,u}m\sin\left(\tan^{-1}\left(\frac{(h_{df}-x_{l,u}-r_{ffl,u})\cos(\psi)-\frac{z\psi\,sin(\psi)}{2}}{(h_{df}-x_{l,u}-r_{ffl,u})\sin(\psi)-\frac{z\psi\,cos(\psi)}{2}}\right)\right)\right\}\right]\sin\left(\pm 2\left(\frac{\frac{\pi}{4}+(h_{df}-r_{ffl,u})\tan(\phi_{l,u})+\frac{r_{ffl,u}}{\cos(\phi_{l,u})}}{z}\right)\right) \mp \left[\frac{\text{mz}\,\psi\cos(\psi)}{2} - \left(\frac{m\left(z-2\left(h_{df}-x_{l,u}-r_{ffl,u}\right)\right)}{2}\right)\sin(\psi) + r_{ffl,u}m\cos\left\{\tan^{-1}\left(\frac{(h_{df}-x_{l,u}-r_{ffl,u})\cos(\psi)-\frac{z\psi\,sin(\psi)}{2}}{(h_{df}-x_{l,u}-r_{ffl,u})\sin(\psi)-\frac{z\psi\,cos(\psi)}{2}}\right)\right\}\right]\cos\left(\pm 2\left(\frac{\frac{\pi}{4}+(h_{df}-r_{ffl,u})\tan(\phi_{l,u})+\frac{r_{ffl,u}}{\cos(\phi_{l,u})}}{z}\right)\right) \quad (70)$$

$$y_{l,u} = \left[\frac{\text{mz}\,\psi\sin(\psi)}{2} + \left(\frac{m\left(z-2\left(h_{df}-x_{l,u}-r_{ffl,u}\right)\right)}{2}\right)\cos(\psi) - \left\{r_{ffl,u}m\sin\left(\tan^{-1}\left(\frac{(h_{df}-x_{l,u}-r_{ffl,u})\cos(\psi)-\frac{z\psi\,sin(\psi)}{2}}{(h_{df}-x_{l,u}-r_{ffl,u})\sin(\psi)-\frac{z\psi\,cos(\psi)}{2}}\right)\right)\right\}\right]\cos\left(\pm 2\left(\frac{\frac{\pi}{4}+(h_{df}-r_{ffl,u})\tan(\phi_{l,u})+\frac{r_{ffl,u}}{\cos(\phi_{l,u})}}{z}\right)\right) \pm \left[\frac{\text{mz}\,\psi\cos(\psi)}{2} - \left(\frac{m\left(z-2\left(h_{df}-x_{l,u}-r_{ffl,u}\right)\right)}{2}\right)\sin(\psi) + r_{ffl,u}m\cos\left\{\tan^{-1}\left(\frac{(h_{df}-x_{l,u}-r_{ffl,u})\cos(\psi)-\frac{z\psi\,sin(\psi)}{2}}{(h_{df}-x_{l,u}-r_{ffl,u})\sin(\psi)-\frac{z\psi\,cos(\psi)}{2}}\right)\right\}\right]\sin\left(\pm 2\left(\frac{\frac{\pi}{4}+(h_{df}-r_{ffl,u})\tan(\phi_{l,u})+\frac{r_{ffl,u}}{\cos(\phi_{l,u})}}{z}\right)\right) \quad (71)$$

It should be noted that when $\phi_u > \phi_l$, x_u must be $\leq x_l$ To avoid interference.

3.5 Computer Aided Geometrical Representations

In this study, to computerize the rack cutter parametric tracing generation method presented in this study, a computer-aided design (CAD) software (SolidWorks Version 2020) has been programmed with the parametric equations that have been derived in this research. Based on the derived parametric equations, the program automatically generated accurate 2D tooth profiles and 3D gear models directly according to the specified design parameter input values (m, z, x_L, x_u, ϕ_L, ϕ_u, r_{ffL}, r_{ffu}). The flowchart in **Fig. 11** illustrates a step-by-step description of the metode procedures. The generated digital file extension is compatible with any CAE or CAM software.

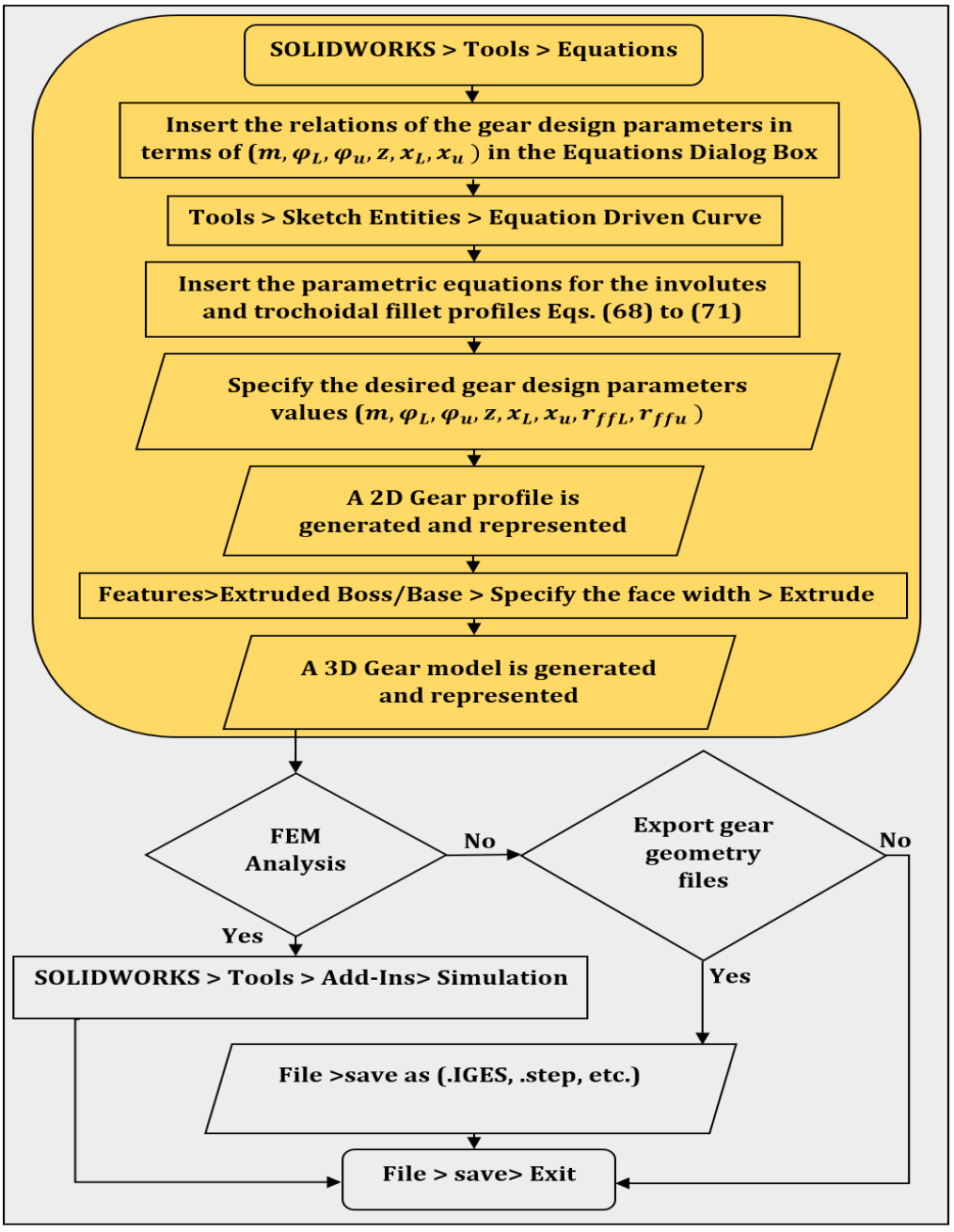

Figure 11. A flowchart showing the computerized generation method's step-by-step procedures.

4. RESULTS AND DISCUSSION

To showcase the capabilities of the computerized rack cutter parametric tracing generation method and the novel asymmetric half-cutter generation techniques presented in this study, the 2D tooth profiles and 3D gear models for several selective samples of standard, asymmetric, nonstandard, and fully asymmetric nonstandard spur gears have been generated according to the procedures described in **Fig. 11**. **Table. 1** lists the design parameters for the selected gear samples. **Figs**. **12** to **16** display the output 2D tooth profiles and 3D gear models for the gear samples. Furthermore, comprehensive comparisons between the proposed generation technique of this work and previous traditional graphical rack-cutter-based generation techniques **(Alaci et al., 2008; Simionescu, 2008; Fetvaci, 2012; Alaci et al., 2022)** have been conducted. **Table 2** summarizes the comparison results. Based on the output results presented in **Figs. 12** to **16** and **Table 2**, it is evident that the computerized generation method and the asymmetric half-cutters generation techniques presented in this paper can efficiently generate 2D tooth geometry and 3D gear models for standard, asymmetric, nonstandard, and fully asymmetric nonstandard spur gears, directly within any CAD software application. It can also provide direct geometry and G-code file extensions for further analysis.

Table. 1. The design parameters number for selective samples of spur gear.

No.	Parameter / Type	ϕ_l Deg.	ϕ_u Deg.	z	m (mm)	x_l	x_u	h_{df}	h_{af}	r_{ffl}	r_{ffu}	F_w (mm)
1	Standard	20^o	20^o	18	4	0	0	1.25	1	0.3	0.3	25
2	Corrected (nonstandard)	14.5^o	14.5^o	14	7	0.5	0.5	1.25	1	0.25	0.25	30
3	Asymmetric pressure angle	20^o	30^o	16	2	0	0	1.25	1	0.28	0.28	15
4	Asymmetric pressure angle and fillets	14.5^o	25^o	8	5	0	0	1.25	1	0.29	0.25	10
5	Fully-asymmetric (nonstandard)	14.5^o	30^o	12	7	0.3	0.2	1.25	1	0.27	0.2	20

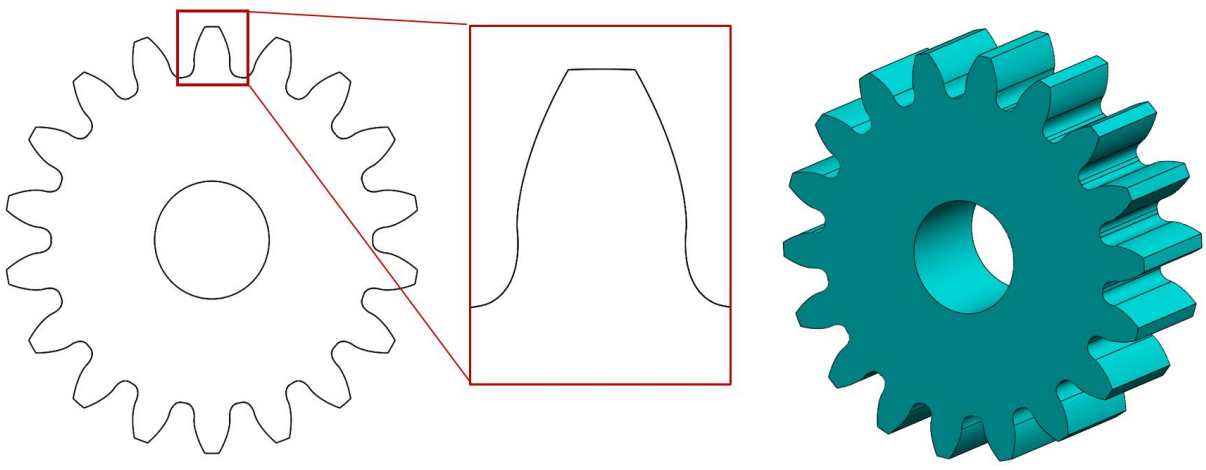

Figure 12. The 2D tooth profile and 3D Model for the standard gear case.

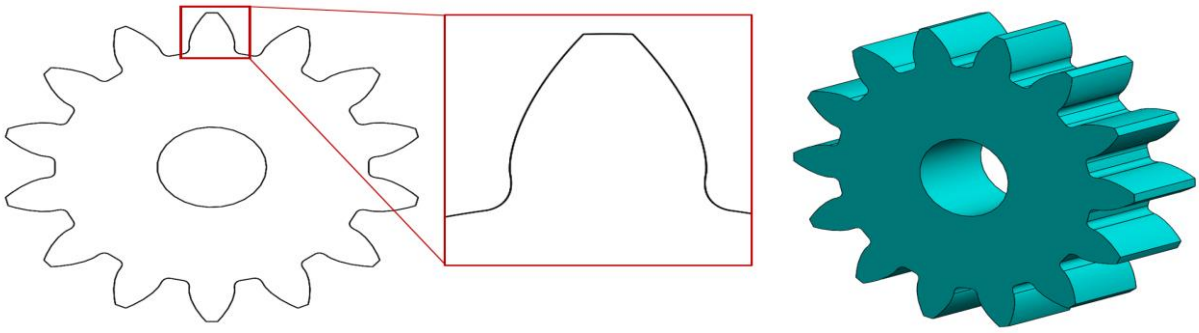

Figure 13. The 2D tooth profile and 3D Model for the corrected gear case.

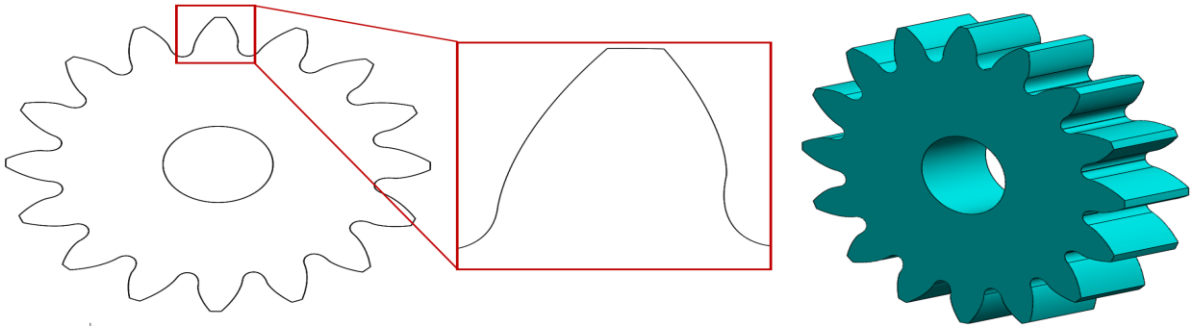

Figure 14. The 2D tooth profile and 3D Model for the asymmetric pressure angle gear case.

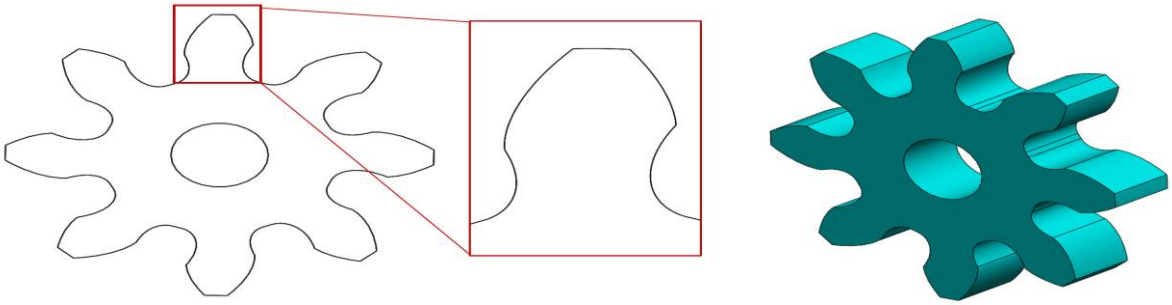

Figure 15. The 2D tooth profile and 3D Model for the asymmetric pressure angle and fillets gear case.

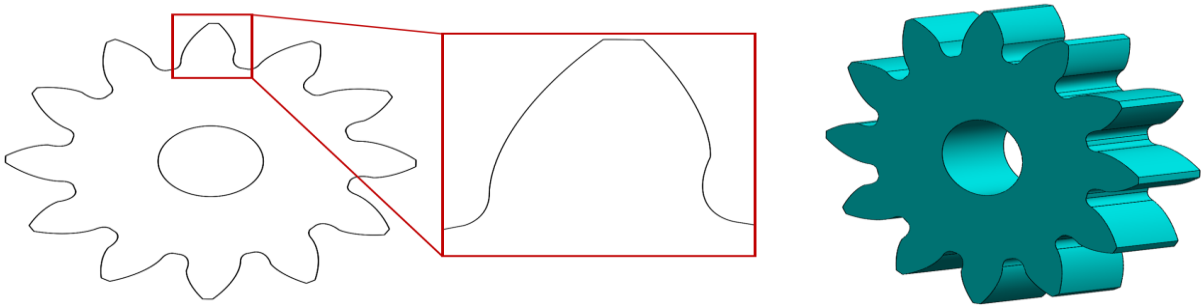

Figure 16. The 2D tooth profile and 3D Model for the fully asymmetric nonstandard gear case.

Table. 2. Comparisons between the proposed generation technique and previous traditional rack-cutter-based generation techniques.

No	Previous rack-cutter-based generation techniques	Current generation method
1	Require a specific source code to be written.	Does not require a source code.
2	Require the use of a programming language.	Does not require a programming language.
3	A graphic processor is required to display computer graphs.	Graphs are directly auto-generated and displayed.
4	A post-graphic processor is required to eliminate the lines and curves that do not belong to the gear tooth geometry **(Alaci et al., 2008)**.	Does not generate lines or curves that do not belong to the gear tooth geometry that is required to be eliminated.
5	Generates 2D gear geometry.	Both 2D and 3D gear geometry can be directly obtained.
6	A more complex mathematical model.	Direct form of parametric equations.
7	No convenient way of exporting the generated geometry to a CAD package **(Simionescu, 2008)**.	Gear geometry is directly generated within the CAD package.
8	A relative tooth profile's accuracy is influenced by the number of simulated cutting process frames.	Since a parametric equation-driven curve generates the tooth profile, its accuracy is absolute.
9	Not directly possible.	Gear geometry files can be directly exported as (.IGES) or (.Step) files to any CAE software.
10	Not directly possible.	Post-FEM analyses can be directly conducted in the same package.
11	Not directly possible.	The G-code of the gear geometry required for the gear manufacturing processes can be directly obtained in the same package.
12	Require numerical solving of a system of equations to calculate the undercutting radius **(Alaci et al., 2022).**	The undercutting radius can be directly estimated utilizing the package tools.
13	More time-consuming as it necessitates the use of source code, a programming language, a graphic processor for displaying computer graphs, a post-graphic processor for eliminating unrelated lines and curves, and a post-process for exporting the tooth geometry to CAD software.	Direct and efficient in terms of time, as it does not necessitate the use of source code, a programming language, a graphic processor for displaying computer graphs, a post-graphic processor for eliminating unrelated lines and curves, or a post-process for exporting the tooth geometry to CAD software. Instead, it generates the gear profile directly in the CAD software, utilizing a variety of modern CAD software capabilities.
14	A single asymmetric rack cutter was utilized to generate asymmetric gear teeth.	Two half-rack cutters have been used to generate the desired asymmetric gear tooth.
15	The physical behavior of the gear under operating conditions can be simulated and investigated **(Fetvaci, 2012)**.	Not directly possible.

5. CONCLUSIONS

In this research, a direct and time-efficient computerized rack cutter generation method is presented. When compared with the traditional graphical rack-cutter-based generation method, the proposed method does not entail the use of a source code, a programming language, a graphic processor for displaying computer graphs, a post-graphic processor for eliminating unrelated lines, or a post-process for exporting the tooth geometry to CAD software. Instead, it efficiently generates accurate gear profiles directly in any CAD software, utilizing a variety of modern CAD software capabilities. The proposed generation method aims to efficiently provide accurate gear geometry files, enabling readers to conduct precise FEM analyses and fabricate accurate gear specimens for experimental testing. Moreover, a novel technique to generate asymmetric gears and fully asymmetric nonstandard spur gears (pressure angle, trochoidal fillet, and shifting factor asymmetries) is proposed using two half-rack cutters, where each half is used to generate one half of the tooth. Furthermore, the parametric equations for the tooth fillets and tooth involute profiles, derived from the parametric tracing of the reciprocal motion between the rack cutter and the gear blank, have been reformulated to account for various gear tooth asymmetries and nonstandard modifications. A CAD program has been programmed with the parametric equations reformulated in this research. Based on these parametric equations, the program automatically generated accurate 2D tooth profiles and 3D gear models. The generated digital file extensions are compatible with any CAE or CAM software. In conclusion, this paper proposes a technique to generate asymmetric gears and fully asymmetric nonstandard spur gears. A computerized rack cutter parametric tracing generation method has been presented as an alternative to the traditional generation method, where A CAD program has been utilized to generate the gear geometry files. However, despite its accuracy and time efficiency, this generation method has some limitations. Specifically, it does not simulate the gear-cutting process, which means that the physical interactions between the gear and the rack cutter during the cutting operation cannot be visualized or analyzed. Nevertheless, the generation techniques proposed in this work can further be extended to generate other gear types, such as helical gears, internal gears, etc.

NOMENCLATURE

Symbol	Description	Symbol	Description
$R_b, R_s \& R_p$	Base, Generation, and pitch radii, mm.	w	Rolling angles, deg.
m	Module, mm.	ϕ & ϕ_s	Pressure angle at pitch radius, deg.
z	No. of teeth.	$\phi_R, \theta_R \&$ ϒ	Construction angles.
x	Profile shift factor.	$\lambda \& \psi$	Generation angle, rad.
$x_{l,r}$ & $y_{l,r}$	Parametric coordinates, mm	l, u	Referred to the loaded or unloaded side.
L, b	Construction lengths, mm.	l, r	Referred to the left or right side.
$t_s, s_s, c \& p$	Circler tooth and space thickness for the gear and rack, respectively, mm.	c , w	Referred to the corrected and working dimension.
$h_{d_f} \& r_{f_f}$	Tooth dedendum and rack fillet arc factors, respectively.	1, 2	Referred to the pinion and gear.

Credit Authorship Contribution Statement

Ahmed A. Toman: Conceptualization, Methodology, Software, Investigation, Writing-original Draft. Mohammad Q. Abdullah: Conceptualization, Supervision, Proofreading.

Declaration of Competing Interest

The authors declare that they have no known competing financial interests or personal relationships that could have appeared to influence the work reported in this paper.

REFERENCES

Abdullah, M. Q, 2016. Enhancement of a gear drive performance using an alternative design approach of teeth profiles. Ph.D. Thesis, Department of Mechanical Engineering, University of Baghdad, Baghdad, Iraq.

Abdullah, M.Q. and Badri, T.M., 2011. Numerical investigation of static and dynamic stresses in spur gear made of composite material. *Journal of Engineering*, 17(04), pp.763–782. https://doi.org/10.31026/j.eng.2011.04.10.

Abdullah, M.Q., and Jweeg, M.J., 2012. Simulation of Generation Process for Asymmetric Involute Gear Tooth Shape with and without Profile Correction. *Innovative Systems Design* and Engineering, 3(6). ISSN 2222-2871.

Abdullah, M.Q., Jameel, A.N. and Hasan, H.S., 2015. Reduction of noise and vibration of spur gear by using asymmetric teeth profiles with tip relief. *Journal of Engineering*, 21(9), pp.105–118. https://doi.org/10.31026/j.eng.2015.09.07.

ALACI, S., AMARANDEI, D., CIORNEI, F.C. and PĂTRAŞ-CICEU, S., 2008. Simulation of gear rack generation of involute spur gears. *Annals of the Oradea University. Fascicle of Management and Technological Engineering*, 7, pp.1172-1180. https://imt.uoradea.ro/auo.fmte/files-2008/TCM_files/ALACI%20STELIAN%201.pdf .

Alaci, S., Ciornei, F.C. and Doroftei, I.A., 2022, October. Proposed gear rack cutter for spur gear manufacturing by generating method. Part II: Comparison between the standard and modified profiles. *In IOP Conference Series: Materials Science and Engineering*, 1262, (1), p. 012040. IOP Publishing. http://dx.doi.org/10.1088/1757-899X/1262/1/012040 .

Barmina, N. and Trubachev, E., 2021. *Gears in Design, Production, and Education*. Springer Nature.

Bhosale, K.C. and Ahmadnagar, D., 2011. Analysis of bending strength of helical gear by FEM. *Innovative Systems Design and Engineering*, *2*(4), pp.125-127.

Buckingham, E., 2011. *Analytical mechanics of gears*. Dover Publications (November 10, 2011).

Chen, C.-F. and Tsay, C.-B., 2005. Tooth profile design for the manufacture of helical gear sets with small numbers of teeth. *International Journal of Machine Tools and Manufacture*, 45(12–13), pp.1531–1541. https://doi.org/10.1016/j.ijmachtools.2005.01.017.

Ciornei, F., Alaci, S., Romanu, I. and Doroftei, I., 2022. Proposed gear rack cutter for spur gear manufacturing by generating method. Part I: Theoretical and strength analysis arguments. *IOP Conference Series. Materials Science and Engineering*, 1262(1), p.012042. https://doi.org/10.1088/1757-899x/1262/1/012042.

Colbourne, J.R., 1987. *The geometry of involute gears*. Springer Science & Business Media.

Davis, J.R. ed., 2005. *Gear materials, properties, and manufacture*. ASM international.

Fetvaci, C. and Imrak, E., 2008. Mathematical model of a spur gear with asymmetric involute teeth and its cutting simulation. *Mechanics Based Design of Structures and Machines*, 36(1), pp.34–46. https://doi.org/10.1080/15397730701735731.

Fetvaci, C., 2012. *Computer simulation of involute tooth generation*. INTECH Open Access Publisher. http://dx.doi.org/10.5772/34079.

Gupta, B., Choubey, A. and Varde, G.V., 2012. Contact stress analysis of spur gear. *International Journal of Engineering Research and Technology*, *1*(4), pp.1-7.

Gupta, K., Kumar, N. Jain and Laubscher, R. 2017. *Advanced gear manufacturing and finishing*: *classical and modern processes*. London: Matthew Deans. ISBN: 9780128045060.

Hassan, A.R., 2018. Pressure angle and profile shift factor effects on the natural frequency of spur tooth design. *International Journal of Mechanical and Mechatronics Engineering*, 12(1), pp.58-64. https://doi.org/10.5281/zenodo.1316397 .

Hassan, A.R.,2008. Static and dynamic stress analysis of Spur gear considering effects of geometric and dynamic parameters.Ph.D. Thesis, Anna University, India. http://hdl.handle.net/10603/29407 .

Hmoad, N.R. and Abdullah, M.Q., 2016. Analytical and numerical tooth contact analysis (TCA) of standard and modified involute profile Spur gear. *Journal of Engineering*, [online] 22(3), pp.111–128. https://doi.org/10.31026/j.eng.2016.03.08.

Hmoad, N.R., 2016. Improvement of sliding velocity behavior and load-carrying capacity for toothed gear by modifying teeth profile geometry. Ph.D. Thesis, Department of Mechanical Engineering, University of Baghdad, Baghdad, Iraq.

Ismail, M.A. and Abdullah, M.Q., 2019. Generation and experimental stress analysis of elliptical gears with combined teeth. *Journal of Engineering*, 25(10), pp.154–171. https://doi.org/10.31026/j.eng.2019.10.11.

Kapelevich, A., 2000. Geometry and design of involute spur gears with asymmetric teeth. *Mechanism and Machine Theory*, 35(1), pp.117–130. https://doi.org/10.1016/s0094-114x(99)00002-6.

Kapelevich, A.L., 2018. *Asymmetric gearing*. CRC Press.

Litvin, F.L., Lian, Q. and Kapelevich, A.L., 2000. Asymmetric modified spur gear drives: reduction of noise, localization of contact, simulation of meshing, and stress analysis. *Computer Methods in Applied Mechanics and Engineering*, 188(1–3), pp.363–390. https://doi.org/10.1016/s0045-7825(99)00161-9.

Lynwander, P., 1983. *Gear drive systems: Design and application*. CRC Press.

Masuyama, T. and Miyazaki, N., 2016. Evaluation of load capacity of gears with an asymmetric tooth profile. *International Journal of Mechanical and Materials Engineering*, 11(1). https://doi.org/10.1186/s40712-016-0064-0.

Masuyama, T., Mimura, Y. and Inoue, K., 2015. Bending strength simulation of asymmetric involute tooth gears. *Journal of Advanced Mechanical Design, Systems, and Manufacturing*, 9(5), p.JAMDSM0071. https://doi.org/10.1299/jamdsm.2015jamdsm0071.

Mitchiner, R.G. and Mabie, H.H., 1982. The determination of the Lewis form factor and the AGMA geometry factor J for external spur gear teeth. *Journal of Mechanical Design*, 104(1), pp.148–158. https://doi.org/10.1115/1.3256305.

Mo, J., Yuan, K., Wang, R., Fu, S., Luo, Y. and Li, Y., 2024. Computerized design, simulation of meshing, and stress analysis of bionic logarithmic spiral spur gear drives. *Journal of Engineering Design*, [online] pp.1–27. https://doi.org/10.1080/09544828.2024.2360388.

Radzevich, S.P., 2016. *Dudley's handbook of practical gear design and manufacture*. CRC press.

Radzevich, S.P., 2017. *Gear cutting tools: science and engineering*. CRC Press.

Rao, P.S. and Vamsi, C., 2016. Contact stress and shear stress analysis of spur gear using Ansys and theoretical. *Int. J. of Modern Studies in Mech. Engineering*, *2*(2). http://dx.doi.org/10.20431/2454-9711.0202002.

Risitano, A., 2011. *Mechanical design*. CRC Press. ISBN-13: 978-1439811696.

Shaoyan, W., and Yufu, L., 2022. *Fundamentals of Mechanical Design*. Dalian University of Technology Press.

Simionescu, P.A., 2008, June. Interactive involute gear analysis and tooth profile generation using working model 2D. *In 2008 Annual Conference & Exposition*, pp. 13-781. http://dx.doi.org/10.18260/1-2--3796 .

Toman, A.A. and Abdullah, M.Q., 2020. An analytical solution for the maximum tensile stress and stress concentration factor investigations for standard, asymmetric fillets, asymmetric pressure angle, and profile helical and spur gears. *Journal of Engineering*, 26(7), pp.217–237. https://doi.org/10.31026/j.eng.2020.07.15.

Ugural, A.C., 2022. *Mechanical design of machine components: SI version*. CRC Press.

Yang, S. C., 2004. Mathematical model of a helical gear with asymmetric involute teeth and its analysis. *International Journal of Advanced Manufacturing Technology*, 26(5–6), pp.448–456. https://doi.org/10.1007/s00170-003-2033-z.

Yılmaz, T.G., Dogan, O. and Karpat, F., 2017, June. Stress analysis of thin-rimmed spur gears with asymmetric trochoid. In *Proc. International Conference on Mechanics and Industrial Engineering*. http://dx.doi.org/10.11159/icmie17.132.

Yılmaz, T.G., Kalay, O. and Karpat, F., 2018. Stress analysis of thin-rimmed asymmetric spur gears. *International Journal of Advances on Automotive and Technology*, *2*(3), pp.143-150. http://dx.doi.org/10.15659/ijaat.18.09.991.

Zhai, G., Liang, Z. and Fu, Z., 2020. A mathematical model for parametric tooth profile of spur gears. Mathematical Problems in Engineering, 2020, pp.1–12. https://doi.org/10.1155/2020/7869315.

Zhang, Y. and Mi, C., 2018. *Automotive power transmission systems*. John Wiley & Sons. ISBN: 9781118964897.

التمثيل الهندسي المحوسب للقطع بالتوليد للمسننات ذات المنحنى المنشأ غير القياسية وغير المتناضرة استنادًا إلى التتبع البارامتري لشفرة الجريدة المسننة

أحمد علي تومان[1,2]*، محمد قاسم عبد الله[1]

[1]قسم الهندسة الميكانيكية، كلية الهندسة، جامعة بغداد، بغداد، العراق
[2]قسم هندسة السيارات، كلية الهندسة المسيب، جامعة بابل، بابل، العراق

الخلاصة

في مجال التصميم الهندسي للمسننات تتطلب عملية اجراء أي نوع من انواع التحري كالتحري بطريقة تحليل العناصر المنتهية والتحري الديناميكي وتحري الاجهادات تمثيل هندسي دقيق لتصميم اسنان المسننات ويجب تجنب أي نوع من انواع التقريب اثناء عملية التمثيل الهندسي. في الأدبيات السابقة تم إجراء العديد من عمليات التقدير والتقريب وخاصة في منطقة منحنى جذر السن، حيث تم تمثيله بخط مستقيم أو قوس دائري بدلاً من تمثيله بمنحنى عجلي ناتج من عملية قطع بالتوليد. قد يؤدي هذا التقريب إلى نتائج إجهادات انحناء غير دقيقة لأنه قد لا يكون من الممكن ملاحظة تأثيرات حالات التقويض في السن أو تأثيرات عمليات التصحيح. لوحظت أيضا في الأدبيات السابقة وعلى نطاق واسع تقديرات أخرى كاستخدام شفرة جريدة مسننة واحدة غير متناظرة لإنشاء جانبي السن من النوع غير المتناظر. علاوة على ذلك، تم ملاحظة استخدام الطريقة الرسومية للتمثيل الهندسي للقطع بالتوليد باستخدام شفرة الجريدة على نطاق واسع. هذه الطريقة على الرغم من دقتها في التمثيل الهندسي للأسنان من النوع القياسي إلا أنها تستغرق وقتًا طويلاً كونها تتطلب كتابة برنامج خاص واستخدام لغة برمجة ومعالج رسومي لعرض الرسوم وعملية معالجة لإزالة الخطوط الإضافية وعملية معالجة أخرى لتصدير ملفات المسننات إلى برامج التصميم والتحليل بالحاسوب. ولذلك يقدم هذا البحث طريقة بديلة ومحوسبة للتمثيل الهندسي للقطع بالتوليد لأنشاء وتمثيل المسننات ولقد تم خلال مجريات البحث اثبات دقتها وقدرتها على التمثيل الهندسي ثنائي وثلاثي الابعاد وبانها أكثر كفاءة من حيث عامل الوقت مقارنة بالطريقة الرسومية التقليدية. تم اقتراح تقنيات جديدة لأنشاء اسنان غير متناظرة من حيث زويا الضغط وجذور السن ومعاملات التصحيح وذلك باستخدام نصفين غير متناظرين من شفرة الجريدة.

الكلمات المفتاحية: التمثيل الهندسي للقطع بالتوليد، التروس ذات المنحنى المنشأ ، غير القياسية، غير المتناضرة ، شفرة الجريدة المسننة.